JOURNAL OF MATERIALS SCIENCE 35 (2000) 5569–5574

Pressureless sintering of SiC-TiC composites with improved fracture toughness

YOUNG-WOOK KIM*, SUNG-GU LEE, YOUNG-IL LEE
Department of Materials Science and Engineering, The University of Seoul, Seoul 130-743, South Korea
E-mail: ywkim@uoscc.uos.ac.kr

Composites of SiC-TiC containing up to 45 wt% of dispersed TiC particles were pressureless sintered to ~97% of theoretical density at temperatures between 1850°C and 1950°C with Al_2O_3 and Y_2O_3 additions. An *in situ*-toughened microstructure, consisted of uniformly distributed elongated α-SiC grains, matrixlike TiC grains, and yttrium aluminum garnet (YAG) as a grain boundary phase, was developed via pressureless sintering route in the composites sintered at ≥1900°C. The fracture toughness of SiC-30 wt% TiC composites sintered at 1900°C for 2 h was as high as 7.8 MPa·m$^{1/2}$, owing to the bridging and crack deflection by the elongated α-SiC grains.

1. Introduction

Composites of SiC-TiC, consisted of finely dispersed TiC grains in a SiC matrix, can be fabricated by hot-pressing with the aid of Al or Al compound and C to a nearly full density at 2000°C [1–4] or with the aid of metal oxides, such as Al_2O_3 and Y_2O_3, at 1850°C [5]. The TiC toughens the SiC matrix by deflecting the cracks, due to the thermal expansion mismatch ($\Delta\alpha = \sim 2.6 \times 10^{-6}$ °C^{-1}) between TiC and SiC [1].

A few reports have been published on *in situ*-toughened SiC-TiC composites. Maupas *et al*. [6, 7] investigated the fracture toughness of the SiC-TiC nanocomposites with needle-like microstructure that were fabricated via chemical vapor deposition (CVD); these researchers reported a maximum toughness value of 6.2 MPa·m$^{1/2}$ in SiC-15 mol% TiC nanocomposites. Chae *et al*. [8] fabricated the SiC-30 wt% TiC composites by hot-pressing with the aid of 10 wt% Cr_3C_2 to 98.5% of theoretical density at 1950°C; their specimens exhibited a maximum toughness value of 6.2 MPa·m$^{1/2}$ in SiC-30 wt% TiC composites. Cho *et al*. [9] also fabricated *in-situ* toughened SiC-30 wt% TiC composites via a two-step process, hot-pressing with the aid of 7 wt% Al_2O_3 and 3 wt% Y_2O_3 at 1850°C for 1 h and subsequently annealing at 1950°C for 6 h; their microstructure consisted of uniformly distributed elongated α-SiC grains, matrixlike TiC grains, and yttrium aluminum garnet (YAG) as a grain boundary phase and their specimens exhibited a higher fracture toughness of 6.9 MPa·m$^{1/2}$ in SiC-30 wt% TiC composites. The presence of elongated α-SiC grains and weak interface boundaries have been identified as the principal elements of effective grain bridging and crack deflection resulting in the increased fracture toughness [9].

The highly, covalently bonded nature of SiC and the presence of inert second phase particles (TiC) in SiC-TiC composites make pressureless sintering difficult without the use of applied pressure. So far, most of the SiC-TiC composites investigated have been fabricated by hot-pressing or by CVD process although pressureless sintering is a more desirable method of fabrication since complex shapes can be made economically. Liquid-phase sintering is one of the promising method to overcome the lower-sinterability of covalently bonded materials and their composites. Clear examples are liquid-phase sintered SiC [10–12] and Si_3N_4-TiN composites [13].

The present paper investigated the preparation of dense SiC-TiC composites by pressureless sintering with the addition of Al_2O_3 and Y_2O_3 as liquid-forming additives. The microstructure was observed by scanning electron microscopy (SEM) and its fracture toughness was evaluated and correlated with the microstructure.

2. Experimental procedure

Commercially available β-SiC (Ibiden Co., Ltd. Nagoya, Japan, grade Ultrafine), TiC (H. C. Starck, Berlin, Germany, grade C. A. S.), Al_2O_3 (99.9% pure, Sumitomo Chemical Co., Tokyo, Japan), and Y_2O_3 (99.9% pure, Shin-Etsu Chemical Co., Tokyo, Japan) powders were used as the starting powders. Four batches of powder were mixed, each containing 88 wt% carbides (SiC and TiC) and 12 wt% oxides (8 wt% Al_2O_3, and 4 wt% Y_2O_3) as sintering additives. The content of TiC powder in those batches was 0, 15, 30, and 45 wt%. All individual batches were milled in ethanol for 24 h using SiC grinding balls after 1 wt% polyethylene glycol addition as a binder. The milled slurry was dried, sieved, and uniaxially pressed into 15 mm-disks with 6 mm-thick at 30 MPa followed by isostatic

* Author to whom all correspondence should be addressed.

pressing at 150 MPa. The green compacts were placed in a graphite crucible, packed with a powder bed, and sintered under Ar atmosphere in a graphite furnace at temperatures between 1800°C and 1950°C for 2 h. The heating rate was 20°C/min and the cooling rate about 30°C/min from the sintering temperature to 1200°C.

Sintered density was determined by the Archimedes method. The theoretical densities of the specimens were calculated according to the rule of mixtures. The microstructures of the sintered specimens were observed by SEM. X-ray diffraction (XRD) using Cu K_α radiation was performed on ground powders. The fracture toughness was estimated by measuring the lengths of cracks that were generated by a Vickers indenter [14]. The variation of fracture toughness with indentation load (*R*-curve-like behavior) was estimated by changing the indentation load over a range of 49–294 N, and the toughness values that were measured in the steady-state region were reported in this study.

3. Results and discussion

3.1. Pressureless sintering

The change of relative density with temperature are shown in Fig. 1. As shown, all specimens sintered at equal to or higher than 1850°C exhibit relative densities of higher than 96%. Al_2O_3 and Y_2O_3 additives in the sintering of SiC are known to form liquid phase by reacting with the surface SiO_2 of SiC and to promote densification through liquid-phase sintering [15–17]. Present results indicate that the Al_2O_3-Y_2O_3 liquid is an effective additive for liquid-phase sintering of SiC-TiC composites. The liquid wets TiC as well as SiC effectively and it has appreciable solubility of SiC at sintering temperatures. Those are necessary conditions for liquid-phase sintering [18]. The highest density was obtained for specimens sintered at 1850°C for 2 h. Despite the relatively large weight losses (3% to 5%, see Fig. 2), it was possible to achieve maximum sintered densities at 1850°C. The decrease in density above 1850°C is thought to be associated with the increase in weight loss due to reactions between carbides (SiC and TiC) and sintering additives, resulting in volatile components [19]. Figs 1 and 2 show that reactions evolving gaseous

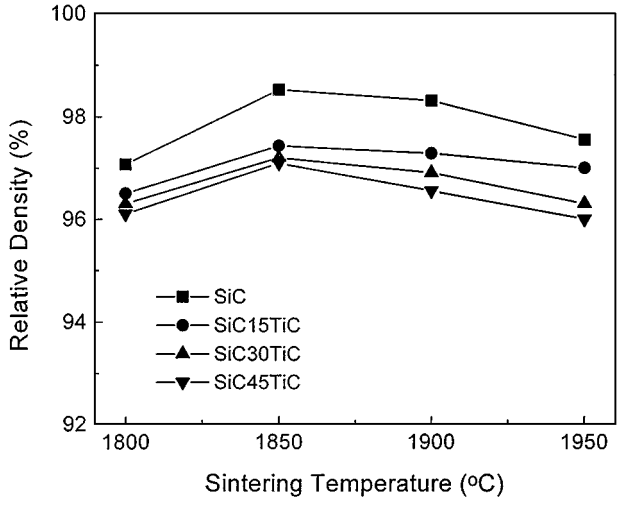

Figure 1 Change of density with sintering temperature for SiC and SiC-TiC specimens containing 8 wt% Al_2O_3 and 4 wt% Y_2O_3.

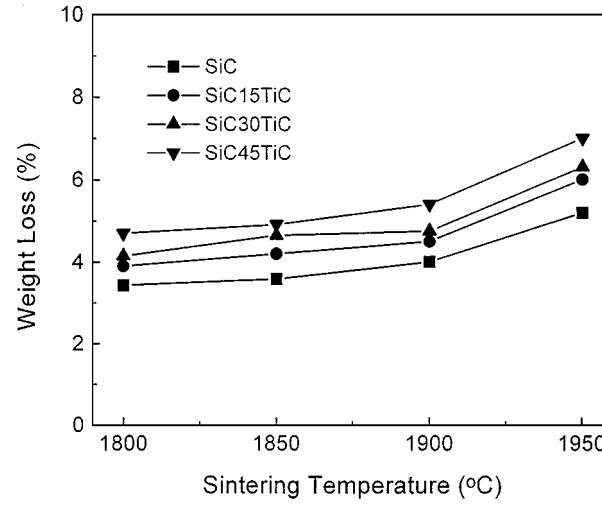

Figure 2 Variation of weight change with sintering temperature for SiC and SiC-TiC specimens containing 8 wt% Al_2O_3 and 4 wt% Y_2O_3.

products compete with densification, resulting in maxima (~97.0% of theoretical) at 1850°C in densities.

Sintered densities of SiC-TiC composites were lower than that of monolithic SiC at all sintering temperatures and decreased with increasing the TiC content. At a given sintering temperature the SiC matrix will sinter much faster than the TiC particle it surrounds. Radial compressive and tensile hoop stresses will therefore develop on the TiC particles upon sintering [20]. Then the densification rate of the composites becomes slower depending on the volume fraction of TiC. If stress relaxation by plastic deformation of TiC and/or creep relaxation by viscous flow of the liquid occur as rapidly as the composites densify, densification is not significantly influenced by the amount of TiC [21]. If, however, deformation and/or creep are much slower, then the densification rate of the composites becomes slower depending on the volume fraction of TiC. Present results suggest that appreciable plastic deformation of TiC and/or creep occur during sintering, however, their rates are slightly slower than the sintering rate, resulting lower sintered density in the composites than in monolithics.

The present results show that SiC-TiC composites can be pressureless sintered at temperatures between 1850°C and 1950°C with Al_2O_3 and Y_2O_3 additions. The high sinter activity of SiC in an Al_2O_3-Y_2O_3 liquid and the ductility of TiC [22], which reduces adverse sintering stress, at sintering temperatures resulted in the successful densification of the SiC-TiC composites. Advantages of using a Al_2O_3-Y_2O_3 liquid phase for sintering of SiC-based composites are as follows: (1) the composites, which are not easily sintered without the aid of pressure, can be sintered to high densities (~97% of theoretical) at temperatures well below 2000°C; (2) SiC and TiC powders with higher oxygen content can be densified; (3) *in-situ* toughened microstructure can be developed by annealing after sintering or sintering at higher temperatures (≥1900°C) (it will be discussed later).

3.2. Microstructure

Fig. 3 shows SEM micrographs of polished surfaces of 1850°C- and 1900°C-sintered specimens with a TiC

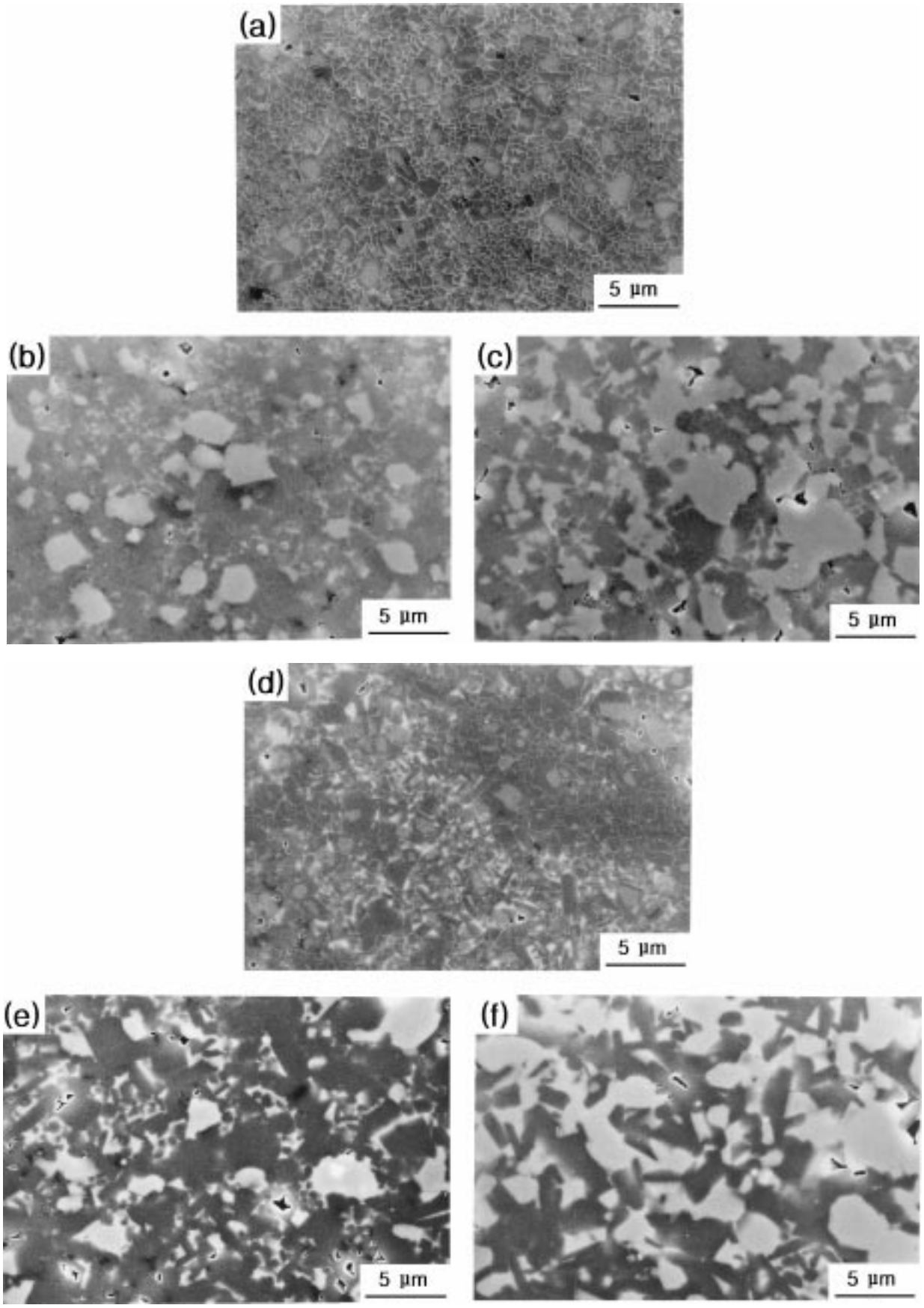

Figure 3 SEM micrographs of polished cross sections of sintered SiC and SiC-TiC composites sintered at 1850°C for 2 h: (a) monolithic SiC, (b) SiC-15 wt% TiC composite, and (c) SiC-45 wt% TiC composite; SiC and SiC-TiC composites sintered at 1900°C for 2 h: (d) monolithic SiC, (e) SiC-15 wt% TiC composite, and (f) SiC-45 wt% TiC composite.

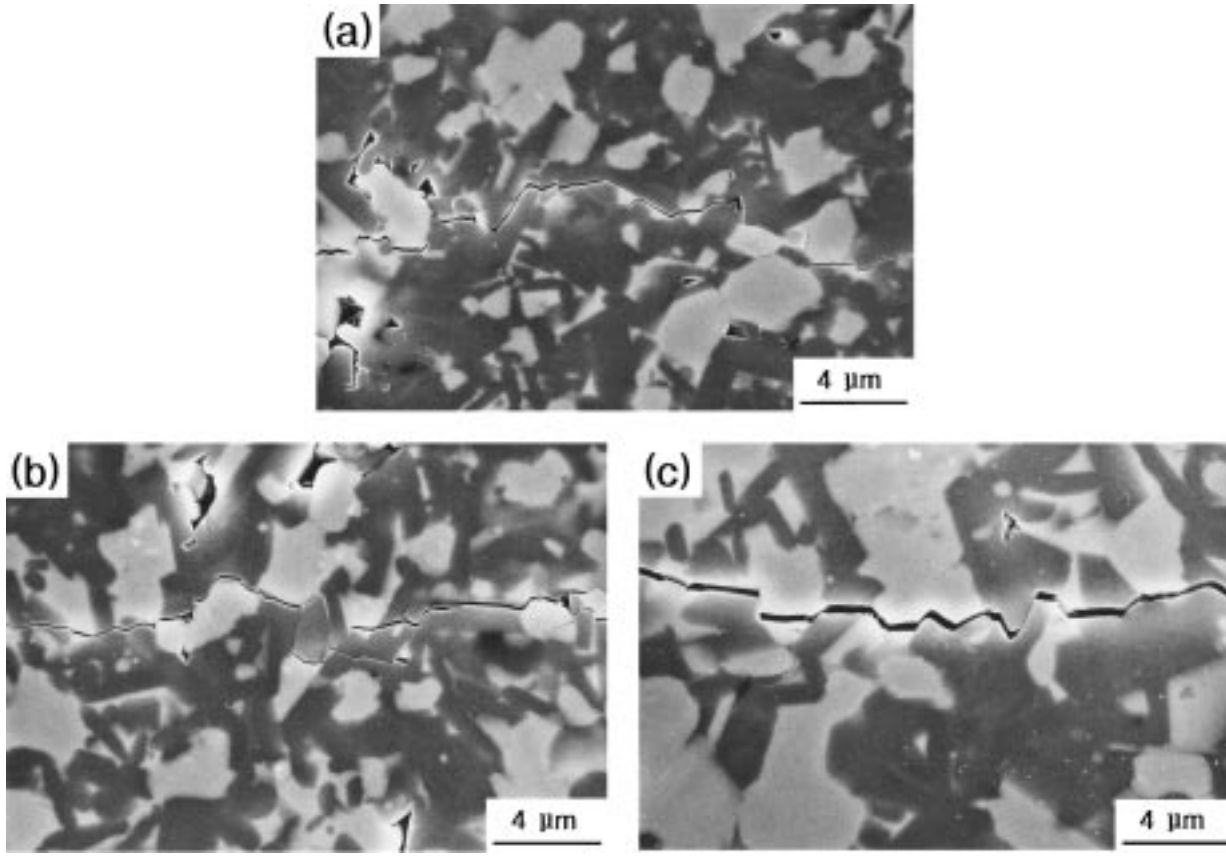

Figure 4 SEM micrographs of crack paths induced by a Vickers indenter for (a) SiC-30 wt% TiC composite sintered at 1900°C for 2 h, (b) SiC-45 wt% TiC composite sintered at 1900°C for 2 h, and (c) SiC-45 wt% TiC composite sintered at 1950°C for 2 h.

content of 0, 15, and 45 wt%. All specimens consist of SiC, TiC, and a small amount of pores. The bright phase is TiC and the grey is SiC. For 1850°C-sintered specimens (Fig. 3a–c), the monolithic SiC was composed mostly of equiaxed grains whose diameters ranged from 0.3 to 1.8 μm. The SiC-TiC composite was a two-phase particulate composite that consisted of randomly distributed TiC grains whose diameters ranged from 0.5 to 5 μm in the relatively fine SiC matrix. The grain size of SiC in the composites (Fig. 3b and c) are similar to the monolithic, indicating that TiC particles do not inhibit the grain growth of SiC.

As shown in Figs 3 and 4, there is a pronounced tendency for grain growth in SiC with increasing sintering temperature. The microstructures of the composites sintered at 1900°C and 1950°C consisted of relatively large, elongated SiC grains and matrixlike TiC grains. *In situ*-toughened composites formed as a result of the grain growth of SiC during sintering. As reported in previous works [9, 23], this kind of microstructure has only been reported in the hot-pressed and subsequently annealed specimens (6-h annealing at 1950°C). However, present results suggest that *in situ*-toughened microstructure can be developed by pressureless sintering in shorter time (2 h-sintering in this work). Phase analysis of the sintered specimens by XRD indicates that $\beta \rightarrow \alpha$ phase transformation, which usually accelerates the grain growth of elongated SiC grains [12], has taken place for sintering temperatures higher than 1850°C. Phase analysis by XRD also shows that all specimens contained a trace of $Y_3Al_5O_{12}$ as a secondary phase. In a previous work [9], the hot-pressing step led to the densification and a minimum grain growth, and the annealing step led to a remarkable grain growth and phase transformation of SiC. In contrast, the pressureless sintering led to the simultaneous occurrence of the densification, the grain growth, and the phase transformation and resulted in faster development of the *in situ*-toughened microstructure. As expected, the elongation of SiC grains, referring to the phase analysis in Table I, is related to the $\beta \rightarrow \alpha$ phase transformation of SiC during sintering. It appears that new α nuclei form and grow inside the β grains during sintering, resulting in α/β composite grains, which we observed in monolithic SiC using high-resolution electron microscopy previously [24]. Strain at the α/β interface accelerates the growth of elongated grains [25]. Though not identified by quantitative image analysis, TiC grains grew with increasing sintering temperatures as well (see Fig. 4b and c). This coarsening may happen by coalescence, as suggested in SiC-TiB_2 composites [26].

One interesting feature is the morphological change of TiC from the equiaxed to the matrixlike with increasing the sintering temperature. The morphological change of TiC appears to occur by plastic deformation of TiC, which is aided by a remarkable sintering pressure, the $\beta \rightarrow \alpha$ phase transformation of SiC, and the ductile nature of TiC during sintering. It suggests that TiC can be deformed easily at the sintering temperature because of its low brittle-ductile transition temperature ($\sim$800°C) [22].

It has been generally established, based on microstructural observation and XRD analysis, that microstructural development in the present system has

TABLE I Properties of some selected monolithic SiC and SiC-TiC composites

No.	Composition (wt%)				Sintering conditions	Relative density (%)	Crystalline phase	
	SiC	TiC	Al_2O_3	Y_2O_3			Major	Trace
1	88		8	4	1850°C, 2 h, Ar	98.5	β-SiC	YAG*, α-SiC
2	58	30	8	4	1850°C, 2 h, Ar	97.2	β-SiC, TiC	YAG, α-SiC
3	88		8	4	1900°C, 2 h, Ar	98.3	α-SiC, β-SiC	YAG
4	58	30	8	4	1900°C, 2 h, Ar	96.9	α-SiC, β-SiC, TiC	YAG
6	88		8	4	1950°C, 2 h, Ar	97.6	α-SiC	β-SiC, YAG
7	58	30	8	4	1950°C, 2 h, Ar	96.3	α-SiC, TiC	β-SiC, YAG

*$Y_3Al_5O_{12}$ (yttrium aluminum garnet).

the following features: (1) *in situ*-toughened SiC-TiC composites can be obtained by pressureless sintering at temperatures equal to or higher than 1900°C; (2) microscopically, the TiC showed a matrixlike morphology while α-SiC showed an elongated morphology in the composites; (3) the $\beta \rightarrow \alpha$ phase transformation of SiC was not hindered by the presence of TiC; (4) the crystallized secondary phase was a $Y_3Al_5O_{12}$ in the composites.

3.3. Fracture toughness

The effects of TiC content and sintering temperature on the fracture toughness of the SiC-TiC composites are shown in Fig. 5. The fracture toughness of 1850°C-sintered specimens increased with increasing the TiC content up to 5.6 MPa·$m^{1/2}$ at 45 wt% TiC loading. In contrast, the composites with *in situ*-toughened microstructure showed maxima in the toughness at 30 wt% TiC loading. For the SiC-30 wt% TiC composites, the fracture toughness increased with increasing the sintering temperature and showed a maximum of 7.8 MPa·$m^{1/2}$ at 1900°C. This value is approximately 75% higher than that of as-hot-pressed composites (4.4 MPa·$m^{1/2}$) reported previously [9]. When the sintering temperature was increased, the shape of the SiC grains changed from equiaxed to elongated, and the average diameter and aspect ratio increased due to the $\beta \rightarrow \alpha$ phase transformation of SiC. Previous results [9] showed that the improved toughness of the *in situ*-toughened SiC-TiC composites was attributed to the enhanced bridging and crack deflection by the elongated SiC grains. All specimens with *in situ*-toughened microstructure investigated herein showed tortuous crack path and demonstrated significant crack deflection and bridging, as shown in Fig. 4. However, higher temperature sintering at 1950°C decreased the toughness slightly from 7.8 to 7.1 MPa·$m^{1/2}$ in the SiC-30 wt% TiC composites, although the length and width of SiC grains increased. This is attributed to the increasing tendency of transgranular fracture of large SiC and TiC grains, as confirmed by separate SEM.

Present results suggest that the SiC-TiC composites with improved fracture toughness can be fabricated by pressureless sintering route and the crack-microstructure interaction behavior of the composite is almost the same with that of the composites fabricated via the hot-pressing and subsequent annealing route.

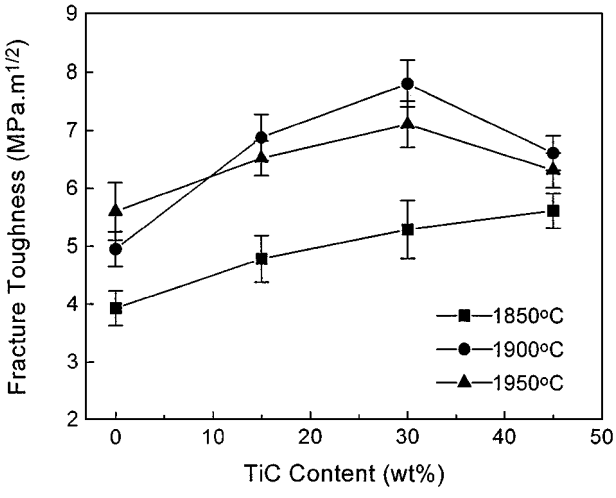

Figure 5 Fracture toughness of the sintered specimens as a function of TiC content.

4. Conclusions

1. SiC-TiC composites containing up to 45 wt% TiC were pressureless sintered with 8 wt% Al_2O_3 and 4 wt% Y_2O_3 additions to ~97% theoretical density at temperatures 1850–1950°C for 2 h.

2. An *in situ*-toughened microstructure, consisted of elongated SiC grains, matrixlike TiC grains, and YAG as a grain boundary phase was developed via pressureless sintering route at temperatures of 1900°C and 1950°C.

3. The room temperature fracture toughness of SiC-30 wt% TiC composites sintered at 1900°C for 2 h in argon were as high as 7.8 MPa·$m^{1/2}$, owing to the bridging and crack deflection by the elongated SiC grains.

Acknowledgment

We gratefully acknowledge helpful discussions with Dr. M. Mitomo (National Institute for Research in Inorganic Materials, Tsukuba, Japan). This work was supported by the Korea Science and Engineering Foundation (KOSEF) under grant No. 98-0300-06-01-3.

References

1. G. C. WEI and P. F. BECHER, *J. Am. Ceram. Soc.* **67** (1984) 571.
2. M. A. JANNEY, *Am. Ceram. Soc. Bull.* **65** (1986) 357.
3. D. L. JIANG, J. H. WANG, Y. L. LI and L. T. MA, *Mater. Sci. Eng.* **A109** (1989) 401.

4. S. JIHONG, J. DONGLIANG, T. SHOUHONG and G. JINGKUN, *J. Hard. Mater.* **4** (1993) 11.
5. K. S. CHO, Y.-W. KIM, H. J. CHOI and J. G. LEE, *J. Mater. Sci.* **31** (1996) 6223.
6. F. GOURBILLEAU, H. MAUPAS, R. HILLEL and J. L. CHERMANT, *Mater. Res. Bull.* **29** (1994) 673.
7. H. MAUPAS, J. L. CHERMANT and R. HILLEL, *ibid.* **29** (1994) 895.
8. K. W. CHAE, K. NIIHARA and D.-Y. KIM, *J. Am. Ceram. Soc.* **79** (1996) 3305.
9. K.-S. CHO, Y.-W. KIM, H.-J. CHOI and J.-G. LEE, *ibid.* **79** (1996) 1711.
10. N. P. PADTURE, *J. Am. Ceram. Soc.* **77** (1994) 519.
11. M. A. MULLA and V. D. KRSTIC, *J. Mater. Sci.* **29** (1994) 934.
12. Y.-W. KIM, M. MITOMO, H. EMOTO and J. G. LEE, *J. Am. Ceram. Soc.* **81** (1998) 3136.
13. H. J. CHOI, K. S. CHO, J. G. LEE and Y. W. KIM, *ibid.* **80** (1997) 2681.
14. G. R. ANSTIS, P. CHANTIKUL, B. R. LAWN and D. B. MARSHALLI, *ibid.* **64** (1981) 533.
15. M. A. MULLA and V. D. KRSTIC, *Am. Ceram. Soc. Bull.* **70** (1991) 439.
16. Y.-K. KIM, H. TANAKA, M. MITOMO and S. OTANI, *J. Ceram. Soc. Jpn.* **103** (1995) 257.
17. Y.-K. KIM, M. MITOMO and J. G. LEE, *ibid.* **104** (1996) 816.
18. W. D. KINGERY, *J. Appl. Phys.* **30** (1959) 301.
19. Y.-W. KIM and J. G. LEE, *J. Am. Ceram. Soc.* **72** (1989) 1333.
20. R. K. BORDIA and R. RAJ, *Adv. Ceram. Mater.* **3** (1988) 122.
21. R. RAJ and R. K. BORDIA, *Acta Metall.* **32** (1984) 1003.
22. G. DAS, K. S. MAZDIYASNI and H. A. LIPSITT, *J. Am. Ceram. Soc.* **65** (1982) 104.
23. K. S. CHO, H. J. CHOI, J. G. LEE and Y.-W. KIM, *J. Mater. Sci. Lett.* **17** (1998) 1081.
24. Y.-W. KIM, M. MITOMO and H. HIROTSURU, *Kor. J. Ceram.* **2** (1996) 152.
25. L. U. OGBUJI, T. E. MITCHELL, A. H. HEUER and S. SHINOZAKI, *J. Am. Ceram. Soc.* **64** (1981) 100.
26. Y. OHYA, M. J. HOFFMANN and G. PETZOW, *ibid.* **75** (1992) 2479.

Received 11 November 1999
and accepted 8 March 2000